



Journal of Advanced Research in Fluid Mechanics and Thermal Sciences

Journal homepage:
https://semarakilmu.com.my/journals/index.php/fluid_mechanics_thermal_sciences/index
ISSN: 2289-7879



Exploring Unsteady Three-Dimensional Casson Fluid Flow through a Stretching Surface with Heat Source/Sink: A Numerical Investigation

Gobburu Sreedhar Sarma^{1,*}, Gobburu Venkata Subbaiah², Ganji Narender¹, Dhonthi Srinivas Reddy³, Dontula Shankaraiah¹, Marla Umakanth⁴

¹ Department of H&S (Mathematics), CVR College of Engineering, Hyderabad, India

² Department of Mathematics, Government College for Men (A), Kadapa, India

³ Department of Mathematics, Vardhaman College of Engineering, Hyderabad, India

⁴ Department of Humanities and Sciences (Mathematics), CMR Engineering College, Hyderabad, India

ARTICLE INFO

Article history:

Received 27 December 2023

Received in revised form 13 May 2024

Accepted 25 May 2024

Available online 15 June 2024

Keywords:

Magneto hydrodynamic; stretching surface; Casson fluid; heat source; viscous dissipation

ABSTRACT

This research aims to examine the effects of a heat source or sink and viscous dissipation on an MHD unsteady three-dimensional Casson fluid flow across a stretched sheet. Using similarity transformations, the governing partial differential equations are transformed into coupled ordinary differential equations, which are then solved numerically in Matlab. The numerical findings for several physical parameters that impact velocity and temperature profiles are described in tables and graphs. The interesting finding are recorded as follows: When the Magnetic parameter increases, the skin friction coefficient increases along x and z directions, but when the Casson parameter lowers, it decreases. The Nusselt number increases with the enhancement of viscous dissipation parameter and heat source or sink parameter. Understanding the behavior of non-Newtonian fluids in the presence of heat transfer is crucial in a number of domains, including chemical engineering, biomechanics, and material processing. These applications might benefit from this kind of study.

1. Introduction

Research on boundary layer problems on a stretched surface has flourished over the last several decades due to the wide range of practical applications it has in the engineering and industrial production sectors. In physics and fluid mechanics, the boundary layer is a relevant term because it describes the layer of fluid inside a restricted region where viscosity effects are strong. In addition, it's a part of the flow field where relative velocity causes the fluid to deform. Each primary fluid has defining characteristics that shape its behaviour in unique ways. The effectiveness of the finished product depends on both the stretching and cooling speeds used during production. It is crucial to keep the stretching rate constant since a rapid shift in stretching affects the final product by causing an abrupt solidification. Crane [1], and Pop and Na [2] first characterized the two dimensional flow

* Corresponding author.

E-mail address: sarma.sreedhar@gmail.com

<https://doi.org/10.37934/arfmts.118.1.116131>

of an incompressible liquid along the stretching surface within the boundary layer. A stretched sheet with varying surface heat flux was the subject of Elbashbeshy's [3] investigation on heat transfer. Salleh *et al.*, [4] investigated the analysis of boundary flow and heat transfer across stretched surfaces with Newtonian heating. Different impacts of the flow via stretching sheet have been explored by many researchers [5-8].

MHD is an acronym for magneto hydrodynamics, which combines the terms magneto for the magnetic field, hydro for water and dynamics for motion. Analysing the magnetic characteristics of an electrically conducting fluid is what the hydro magnetic flow is doing in the meanwhile. Magneto fluids include plasmas, liquid metals, seawater and electrolytes. A broad variety of technical equipment, including blood pumping machines, heat exchanger designs, and MHD electric power generators, use MHD flow. The primary function of the magnetic parameter in the flow field is to provide a resistive force that keeps the flow going and prevents the boundary layer from separating. Many scholars looked at the flow models that included hydro magnetic phenomena. Furthermore, the MHD flow of Casson fluid along a stretched sheet was studied by Reddy *et al.*, [9]. Faraz *et al.*, [10] shown that MHD effects do have an impact on the axisymmetric flow of the Casson nanofluid. The radiation effect was examined by Sarma *et al.*, [11], whereas the magneto hydrodynamic flow under slip conditions was researched by Hayat *et al.*, [12]. The characteristics of magnetic dipole for shear thinning Williamson nanofluid was studied by Khan *et al.*, [13]. Tabrez and Khan [14] were explored the physical significance of viscous dissipation and magnetic dipole for ferromagnetic nanofluids. MHD Casson nanofluid flow through an inclined stretching sheet with different effects were examined by Sreedhar Sarma *et al.*, [15].

Unsteady flow is defined as a flow that varies with time. It's important to consider unsteady flow effects in engineering design to ensure the system can handle transient conditions and prevent undesirable consequences like pressure surges, cavitation or structural damage. Naganthran and Nazar [16] investigated the time dependent boundary layer flow of a Casson fluid through a stretching sheet. The effect of radiative heat transfer of an unsteady Casson liquid was investigated by Krishanan *et al.*, [17]. Hafidzuddin *et al.*, [18] considered the generalized slip velocity. Numerous researchers have also looked at how an induced magnetic field affects the time-dependent MHD flow in the boundary layer [19-22]. Radiation is caused by a difference in temperature between the surrounding environment and the ambient fluid. The time-dependent natural convection flow of a Casson fluid with thermal radiative flux under various wall constraints was studied by Anwar *et al.*, [23]. The influence of thermal solutal stratifications and activation energy on time dependent polymer nanofluid was explored by Hussain and Khan [24]. Khan [25] was also analysed the effect of time dependent heat and mass transfer for magnetized Sutter by nanofluid flow.

Non-Newtonian fluids are distinguished by their complex stress-strain behaviour. As a result of its usefulness in a variety of technical and industrial contexts, non-Newtonian fluids have garnered an abundance of interest in recent years. The Casson fluid is utilised extensively in many industries, including metalworking, food processing, and many others. The characteristics of yield stresses are seen in Casson fluid. The fluid becomes more like a liquid when the shear stress is greater than the yield stress. For similar reasons, fluids behave like solids when shear stress are smaller than yield stresses. Casson fluids include such common items as jelly, shampoo, ketchup, honey, soup and juice. Any analysis of complex structured fluids must include a study of yield stress. Ashraf *et al.*, [26] examined the Casson fluid within the porous medium with magnetic effect through a non-linear stretching sheet. Later the study of time dependent Casson fluid flow using finite element method was done by Khader *et al.*, [27]. Later, a number of studies investigated the effects of unsteady Casson fluid flow in porous media [28-30]. Maleque [31] looked at the MHD movement of Casson liquid along a revolving disc. The hydro magnetic flow of Casson liquid through porous material was investigated

by Kataria and Patel [32], who took rising wall temperature with heat and mass transfer into consideration. The effects of Hall, DuFour, and thermal radiation on the MHD Casson fluid were studied by Vijayaragavan and Karthikeyan [33]. Numerical treatment of heat transfer characteristics of microchannel heat sink was analysed by Loon *et al.*, [34] and finally Khan *et al.*, [35] studied the importance of heat generation in chemically reactive flow with respect to convective heat surface.

Motivated by the above literature, the purpose of this study is to extend the work of Prashu and Nandkeolyar [36] to examine the characteristics of magneto hydrodynamic unsteady three dimensional flow of Casson fluid through a stretching sheet. The analysis includes the effects of viscous dissipation and heat source or sink. By using the similarity transformations, the governing non-linear partial differential equations were converted into non-linear ordinary differential equations which were solved using a numerical algorithm in Matlab. The impact of different parameters was presented through graphs and tables.

2. Mathematical Analysis

The 3D time-dependent magneto hydrodynamic flow across a linearly stretchable surface of an incompressible Casson fluid has been examined. As the fluid is confined along the positive y -axis direction and the surface is along the plane $y=0$, both have been considered. The sheet is also thought to be stretched along the x -axis. It has been assumed that the time-dependent magnetic field behaves along the y -axis, which is perpendicular to the sheet's surface. In Figure 1, the physical model of flow is shown. Here, the surface temperature is T_w , the ambient temperature is T_∞ and in the x -direction, u_w represents the stretching sheet velocity. The PDEs for the continuity equation, momentum, and energy transfer are included in the system of equations that describes the flow and is provided below [36].

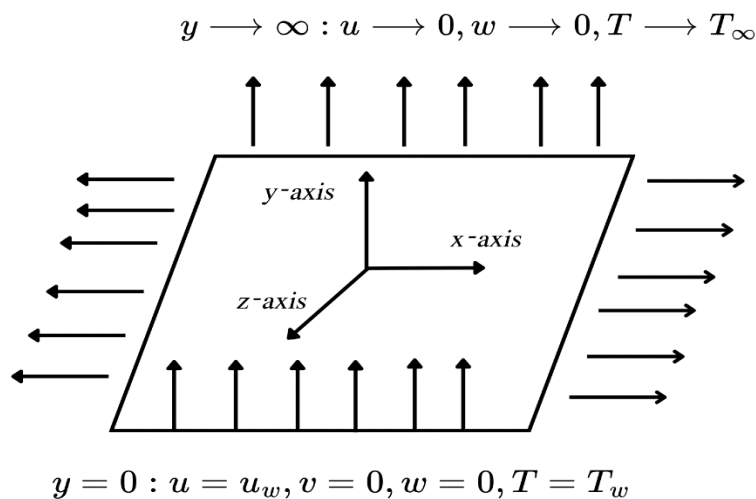


Fig. 1. Physical diagram

$$\frac{\partial u}{\partial x} + \frac{\partial u}{\partial y} + \frac{\partial u}{\partial z} = 0 \tag{1}$$

$$\frac{\partial u}{\partial t} + \frac{\partial u}{\partial x} u + \frac{\partial u}{\partial y} v + \frac{\partial u}{\partial z} w = \nu \left(1 + \frac{1}{\beta}\right) \left(\frac{\partial^2 u}{\partial y^2}\right) - \frac{\sigma B^2(t)}{\rho(1+m^2)} (u + mw), \tag{2}$$

$$\frac{\partial w}{\partial t} + \frac{\partial w}{\partial x} u + \frac{\partial w}{\partial y} v + \frac{\partial w}{\partial z} w = \nu \left(1 + \frac{1}{\beta}\right) \left(\frac{\partial^2 w}{\partial y^2}\right) - \frac{\sigma B^2(t)}{\rho(1+m^2)} (mu - w), \tag{3}$$

$$\frac{\partial T}{\partial t} + \frac{\partial T}{\partial x} u + \frac{\partial T}{\partial y} v + \frac{\partial T}{\partial z} w = -\frac{\nu}{\rho} \left(1 + \frac{1}{\beta}\right) \left(\frac{\partial u}{\partial y}\right)^2 + \alpha_m \left(\frac{\partial^2 T}{\partial y^2}\right) - \frac{1}{\rho c_p} \frac{\partial q_r}{\partial y} - \frac{Q_o}{\rho c_p} (T - T_\infty) \quad (4)$$

The corresponding boundary conditions are

$$\left. \begin{aligned} y = 0: u = u_w(x), v = 0, w = 0, T = T_w \\ y \rightarrow \infty: u \rightarrow 0, w \rightarrow 0, T \rightarrow T_\infty \end{aligned} \right\} \quad (5)$$

β - Casson liquid parameter, σ - electrical conductivity, ρ - density, ν - kinematic viscosity, m - Hall current, T - temperature, $\alpha_m = \frac{k}{\rho c_p}$ the thermal diffusivity. The time dependent wall stretching

velocity by $u_w(x, t) = \frac{ax}{1-\gamma t}$ and the magnetic field with time dependent by $B(t) = B_0(1-\gamma t)^{-\frac{1}{2}}$

where a and γ are constants and B_0 the magnetic strength. Q_o is the volumetric heat source/ sink [23,36].

The radiative heat flux q_r is calculated as [36]

$$q_r = -\frac{4\sigma^*}{3\alpha^*} \frac{\partial T^4}{\partial y} = -\frac{16\sigma^*}{3\alpha^*} T^3 \frac{\partial T}{\partial y} \quad (6)$$

Rosseland mean absorption coefficient is α^* in this case, while the Stefan-Boltzmann constant is σ^* . Substituting q_r in Eq. (4), we get

$$\frac{\partial T}{\partial t} + \frac{\partial T}{\partial x} u + \frac{\partial T}{\partial y} v + \frac{\partial T}{\partial z} w = -\frac{\nu}{\rho} \left(1 + \frac{1}{\beta}\right) \left(\frac{\partial u}{\partial y}\right)^2 + \frac{\partial}{\partial y} \left[\left(\alpha_m + \frac{16\sigma^* T^3}{3\alpha^* \rho c_p} \right) \frac{\partial T}{\partial y} \right] - \frac{Q_o}{\rho c_p} (T - T_\infty) \quad (7)$$

Using the following similarity transformation, the mathematical model Eq. (1) to Eq. (4) may be transformed into a dimensionless [36],

$$u = \frac{ax}{1-\gamma t} f'(\eta), v = -\sqrt{\frac{av}{1-\gamma t}} f(\eta), w = \frac{ax}{1-\gamma t} g(\eta), \theta(\eta) = \frac{T-T_\infty}{T_w-T_\infty}, \eta = y \sqrt{\frac{a}{\nu(1-\gamma t)}} \quad (8)$$

The governing model is reduced to its dimensionless form, which is

$$\left(1 + \frac{1}{\beta}\right) f'''' + f f'' - (f')^2 - A \left(f' + \frac{\eta}{2} f''\right) - \frac{M}{1+m^2} (f' + m g) = 0, \quad (9)$$

$$\left(1 + \frac{1}{\beta}\right) g'' - g f' + f g' - A \left(g + \frac{\eta}{2} g'\right) + \frac{M}{1+m^2} (m f' - g) = 0, \quad (10)$$

$$\left[1 + \frac{4}{3N_r} (1 + (tr - 1)\theta)^3\right] \theta'' - Pr A \frac{\eta}{2} \theta' + Pr f \theta' + Pr \left(1 + \frac{1}{\beta}\right) Ec (f'')^2 + \left[\frac{4}{3N_r} (tr - 1)(1 + (tr - 1)\theta)^2\right] (\theta')^2 + Q \theta(\eta) = 0, \quad (11)$$

The reduced boundary conditions Eq. (5) are

$$f(\eta) = 0, f'(\eta) = 1, g(\eta) = 0, \theta(\eta) = 1 \text{ when } \eta = 0$$

$$f'(\eta) \rightarrow 0, g(\eta) \rightarrow 0, \theta(\eta) \rightarrow 0 \text{ when } \eta \rightarrow \infty \quad (12)$$

The various parameters used in Eq. (9) to Eq. (11) are described below:

$$A = \frac{\gamma}{a}, M = \frac{\sigma B_0^2}{\rho a}, N_r = \frac{k\alpha^*}{4\sigma^* T_\infty^3}, Pr = \frac{\nu}{\alpha_m}, tr = \frac{T_w}{T_\infty}, Ec = \frac{a^2 x^2}{\alpha c_p (T_w - T_\infty)}, Q = \frac{Q_0}{\rho c_p} \quad (13)$$

The following defines the local Nusselt number and the skin friction coefficient along x and z - axes.

$$C_{fx} = \frac{\tau_{wx}}{\rho u_w^2}, C_{fz} = \frac{\tau_{wz}}{\rho u_w^2}, Nu_x = \frac{xq_w}{k(T_w - T_\infty)} \quad (14)$$

Given below are the formulae for τ_w , q_w and q_m .

$$\tau_{wx} = \mu \left(1 + \frac{1}{\beta}\right) \left(\frac{\partial u}{\partial y}\right)_{y=0}, \tau_{wz} = \mu \left(1 + \frac{1}{\beta}\right) \left(\frac{\partial w}{\partial y}\right)_{y=0}, q_w(x) = -k \left(\frac{\partial T}{\partial y} - \frac{q_r}{k}\right)_{z=0} \quad (15)$$

The aforementioned formulas have been transformed into dimensionless form as follows:

$$C_{fx}\sqrt{Re_x} = \left(1 + \frac{1}{\beta}\right) f''(0), C_{fz}\sqrt{Re_x} = \left(1 + \frac{1}{\beta}\right) g'(0),$$

$$\frac{Nu_x}{\sqrt{Re_x}} = - \left[1 + \frac{4}{3N_r} (1 + (t-1)\theta(0))^3\right] \theta'(0) \quad (16)$$

where $Re_x = \frac{xu_w}{\nu}$ is the local Reynolds number, τ_{wx} and τ_{wz} are the shear stress components, q_w - the heat transfer rate.

3. Numerical Solution

The Bvp4c solver in Matlab is used to find numerical solutions for the ODEs Eq. (9) to Eq. (11) that are subject to the BCs Eq. (12). The solver is a method for finite differences with fourth order precision that implements the three-stage Lobatto IIIa formula. To approximate the solution, it uses a collocation technique. The process of collocation entails discretizing the domain into a collection of collocation points and then fulfilling the ODEs at each of these points. The solver iteratively adjusts the solution until it satisfies both the differential equations and the boundary conditions within a specified tolerance. To put the solver into practice, the coupled ODEs Eq. (9) to Eq. (11) are transformed into a system of first-order ODEs in the following way.

Let

$$f = h_1, f' = h_2, f'' = h_3, g = h_4, g' = h_5, \theta = h_6, \theta' = h_7$$

$$h_1' = h_2,$$

$$h_2' = h_3,$$

$$h_3' = \frac{\beta}{1+\beta} \left[A \left(h_2 + \frac{\eta}{2} h_3 \right) - h_1 h_3 + h_2^2 + \frac{M}{1+m^2} (h_2 + m h_4) \right],$$

$$h_4' = h_5,$$

$$h_5' = \frac{\beta}{1+\beta} \left[A \left(h_4 + \frac{\eta}{2} h_5 \right) + h_4 h_2 - h_1 h_5 - \frac{M}{1+m^2} (m h_2 - h_4) \right],$$

$$h_6' = h_7,$$

$$h_7' = \frac{1}{\left(1 + \frac{4}{3R}\right) (1 + (tr-1)h_6)^3} \left[\text{Pr} A \frac{\eta}{2} h_6' - \text{Pr} h_1 h_6' - \text{Pr} \left(\frac{\beta}{1+\beta} \right) E c h_3 - \left(\frac{4}{3R} (tr-1) (1 + (tr-1)h_6)^2 \right) h_7^2 - Q h_6 \right] \quad (17)$$

and the corresponding boundary conditions are

$$h_1(0) = 0, h_2(0) = 1, h_4(0) = 0, h_6(0) = 0,$$

$$h_2(\eta) \rightarrow 0, h_4(\eta) \rightarrow 0, h_6(\eta) \rightarrow 0 \quad \text{as } \eta \rightarrow \infty$$

4. Results and Discussion

Graphs and tables have been used to demonstrate the physical impacts of important parameters on the skin friction and Nusselt number. The spectral quasi linearization technique was used by Prashu and Nandkeolyar [36] to solve the model numerically. The Matlab bvp4c solver has been used for the current survey in order to replicate the solution.

Table 1 presents the findings that highlight the influence of significant parameters on the skin friction coefficients $-C_{fx} \text{Re}^{\frac{1}{2}}$, $-C_{fz} \text{Re}^{\frac{1}{2}}$ and the Nusselt number $Nu_x \text{Re}^{\frac{1}{2}}$. There is a strong agreement between the findings and those of Prashu and Nandkeolyar [36]. The skin friction coefficients grow in both the x and z directions as the value of M rises, but the Nusselt number falls. The ascending values of the Casson parameter β cause the skin friction coefficient to drop in the x and z directions as well as the Nusselt number. Additionally, when the Hall current m accelerates, $-C_{fx} \text{Re}^{\frac{1}{2}}$ decreases and $-C_{fz} \text{Re}^{\frac{1}{2}}$ and the Nusselt number rises. Similarly, when the unsteadiness parameter A values climb, there is a little rise along the x -axis and a drop along the z

-axis in the skin friction coefficient. The decrement in $Nu_x Re^{\frac{1}{2}}$ is observed when A grows. Comparison of present result with Prashu and Nandkeolyar [36] for Nusselt number by varying Magnetic parameter M is depicted in Figure 2.

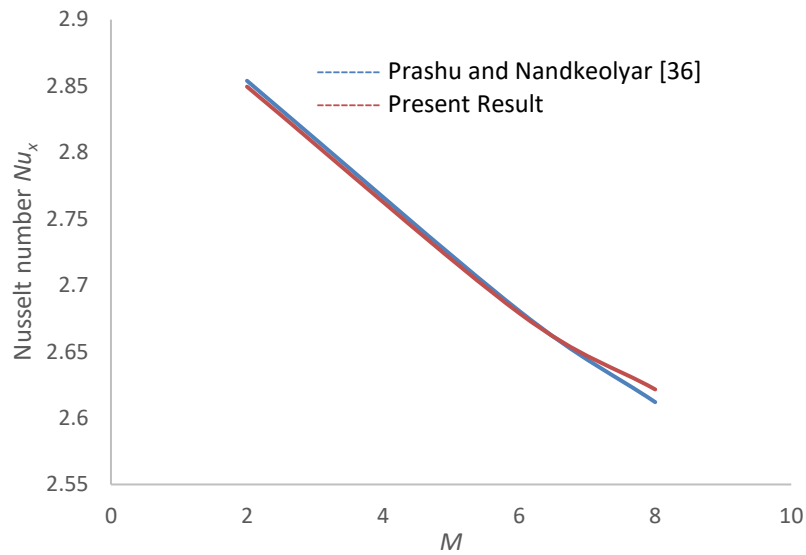


Fig. 2. Comparison of results for Nusselt number with varying M

Table 1

Results of the $-C_{f_x} Re^{\frac{1}{2}}$, $-C_{f_z} Re^{\frac{1}{2}}$ and $Nu_x Re^{-\frac{1}{2}}$ for various parameters

M	m	A	R	tr	β	Pr	$-C_{f_x} Re^{\frac{1}{2}}$		$-C_{f_z} Re^{\frac{1}{2}}$		$Nu_x Re^{-\frac{1}{2}}$	
							Prashu and Nandkeolyar [36]	Present Result	Prashu and Nandkeolyar [36]	Present Result	Prashu and Nandkeolyar [36]	Present Result
6	0.1	0.1	2	1	0.3	10	5.51874	5.51875	0.239056	0.239053	2.680739	2.68074
2							3.63997	3.64076	0.125176	0.124865	2.853953	2.85384
8							6.24973	6.24974	0.279886	0.279885	2.611975	2.61198
	0.5						5.51310	5.51309	1.038104	1.0381	2.709701	2.7097
	1.0						4.47154	4.47148	1.509685	1.50977	2.766775	2.76679
		0.13					5.52749	5.5275	0.238664	0.238661	2.643034	2.64303
		0.15					5.53332	5.53333	0.238403	0.2384	2.617320	2.61732
			4				5.51874	5.51875	0.239053	0.239053	2.446145	2.44614
			6				5.51874	5.51875	0.239053	0.239053	2.358626	2.35863
				2			5.51874	5.51875	0.239053	0.239053	3.863248	3.86325
				3			5.51874	5.51875	0.239053	0.239053	5.082558	5.08255
					0.5		4.59187	4.59187	0.198907	0.198907	2.579187	2.57594
					0.6		4.32925	4.32926	0.187531	0.187532	2.540835	2.53767
						15	5.51874	5.51875	0.239053	0.239053	3.398092	3.39809
						20	5.51874	5.51875	0.239053	0.239053	4.001888	4.00189

The implications of the significant parameters on the Nusselt number are seen in Table 2. Due to accelerating values of the Heat source or sink parameter Q and Viscous dissipation Ec , a rising pattern is seen in the $Nu_x Re^{-\frac{1}{2}}$.

Table 2

Variation of the Nusselt number $Nu_x Re^{-\frac{1}{2}}$ with Ec and Q when $m=0.1, A=0.1, R=2, \beta=0.3, tr=1, Pr=10, M=6$

Ec	Q	$Nu_x Re^{-\frac{1}{2}}$
0.5		7.23144
1		17.1129
2		36.8759
	-0.1	7.12587
	0	7.21108
	0.1	7.29784
	0.2	7.31891

The implications of numerous parameters on velocity and temperature are shown in Figure 3 to Figure 5 respectively. The declining trend of velocity in the x direction due to an increase in β and M values is shown in Figure 3. The characteristics of yield stress are really revealed by the β .

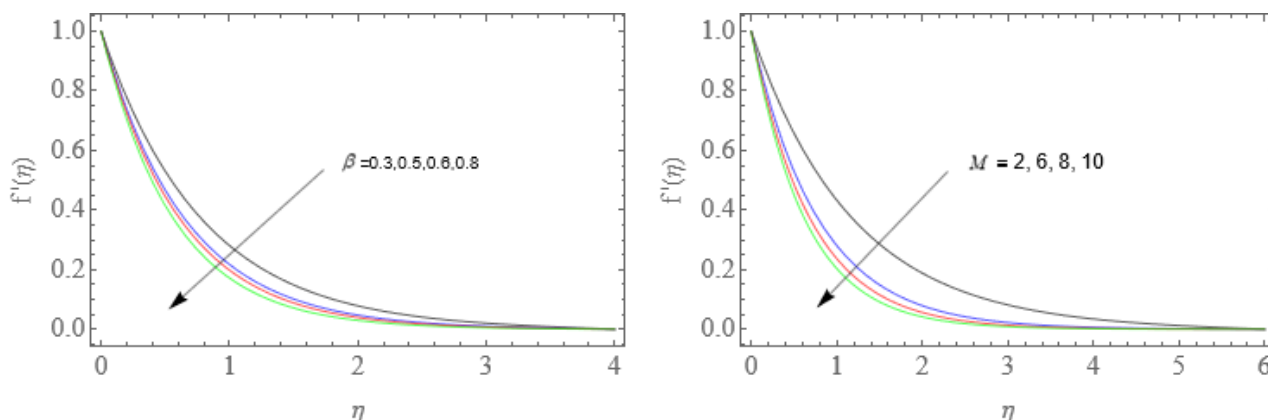


Fig. 3. Change in $f'(\eta)$ for increasing values of β and M

Increasing the yield stress also has stabilizing effects. The Lorentz force in a flow field is a resistive force is created by the effects of an applied magnetic field. Figure 4 illustrates how the velocity profile along the z -axis grows close to the boundary surface before beginning to decrease away from it due to rising values of the Casson parameter β and the magnetic field M . As seen in Figure 5, the temperature profile rises with rising values of M and falls with rising values of β .

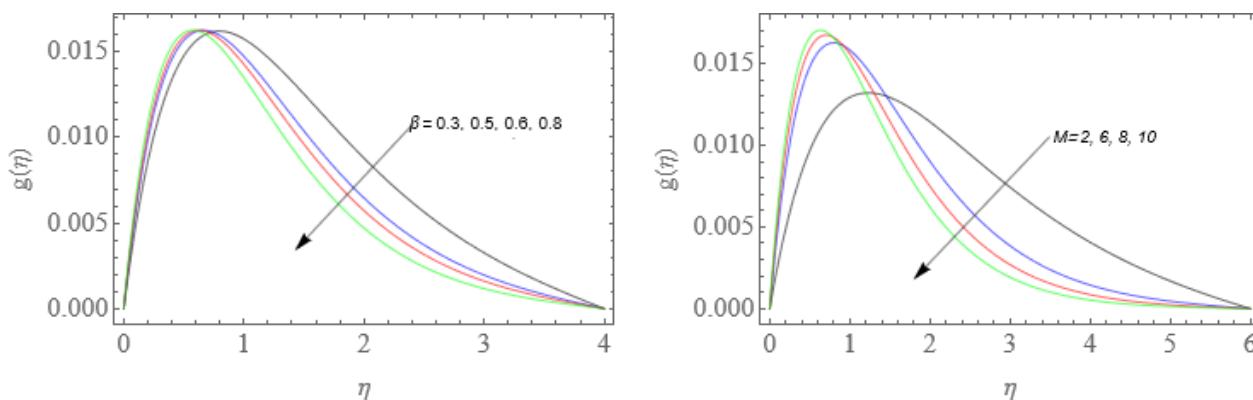


Fig. 4. Change in $g(\eta)$ for increasing values of β and M

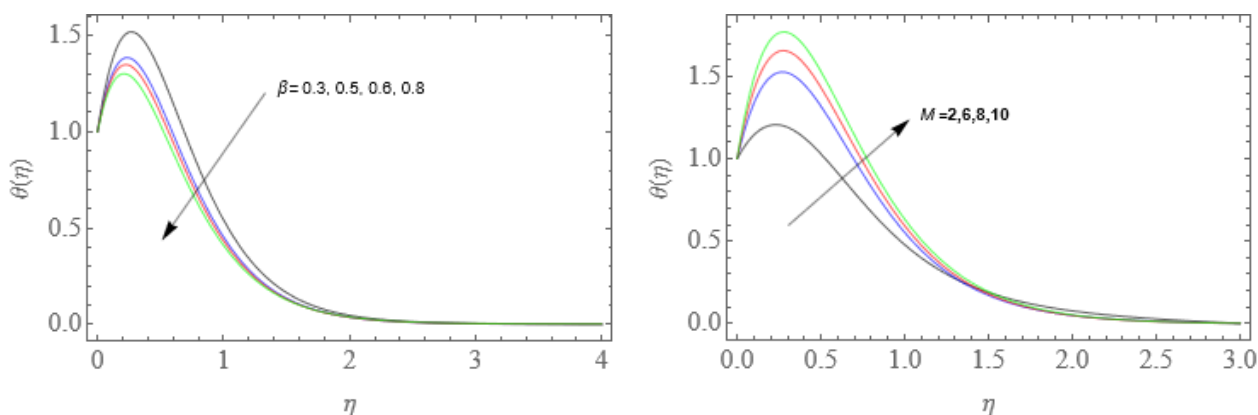


Fig. 5. Change in $\theta(\eta)$ for increasing values of β and M

The influence of significant parameters on velocity and temperature profiles, such as the Hall Current m and the unsteadiness parameter A , is also shown in Figure 6 to Figure 8. Since Hall current is created when an electrically conducting fluid is utilized in combination with a magnetic field, its effects are impossible to ignore when the magnetic field is strong enough. The influence of m and the unsteadiness A on the velocity profile in the x -direction are shown in Figure 6(a) and Figure 6(b). When m values rise, the velocity profile likewise rises. However, when unsteadiness A values rise, the velocity profile marginally declines. The effect of the m and the A on the velocity profile in the z direction is seen in Figure 7(a) and Figure 7(b).

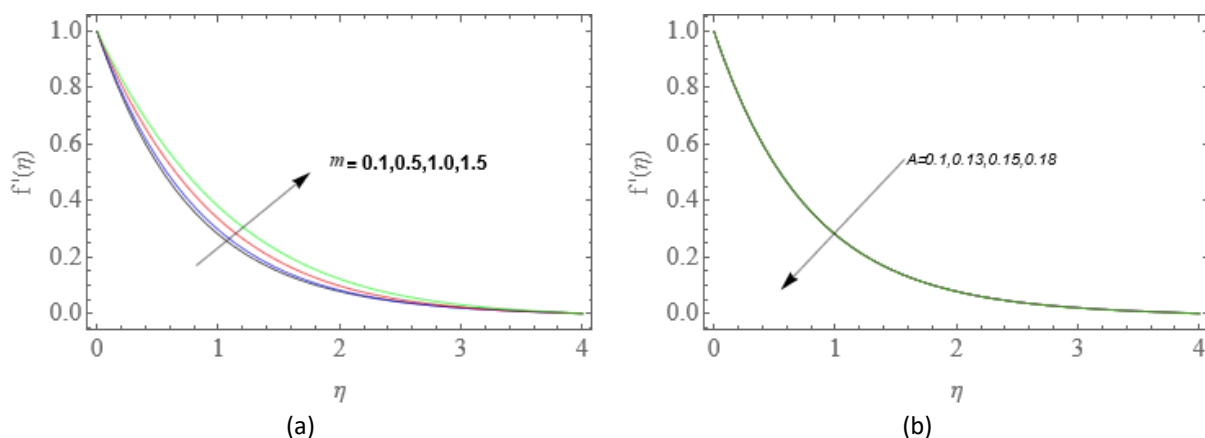


Fig. 6. Change in $f'(\eta)$ for increasing values of m and A

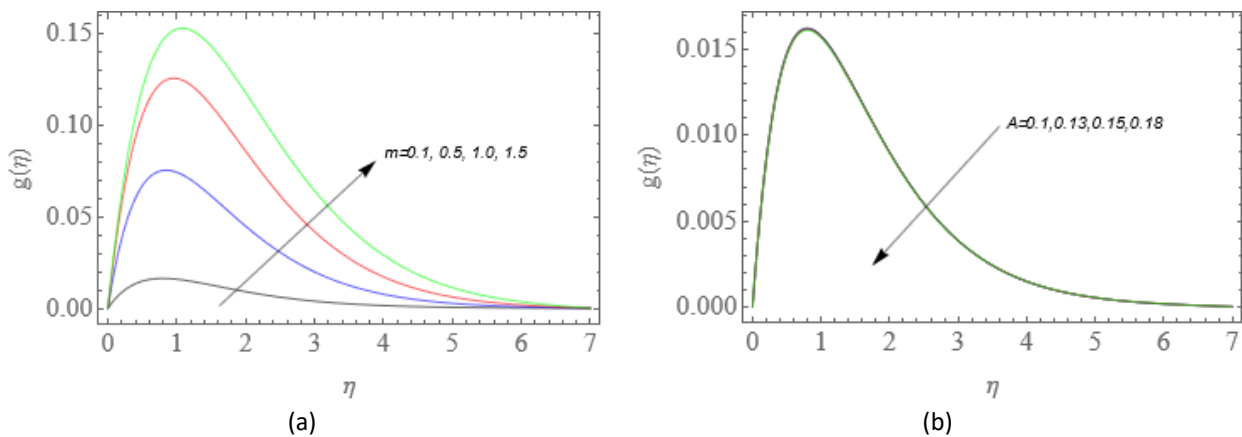


Fig. 7. Change in $g(\eta)$ for increasing values of m and A

There is a slight decrease in the velocity within the boundary layer area for rising values of A , but a considerable increase in the velocity profile for growing values of m . The effect of the m and the A on the temperature is seen in Figure 8(a) and Figure 8(b). However, the temperature is a decreasing function of the Hall current m , and the temperature behaviour is marginally enhanced by raising the values of the unsteadiness A . The momentum boundary layer's thickness is observed to decrease with increasing Hall current m values. However, the thermal boundary layer thickens as unsteadiness A values accelerate.

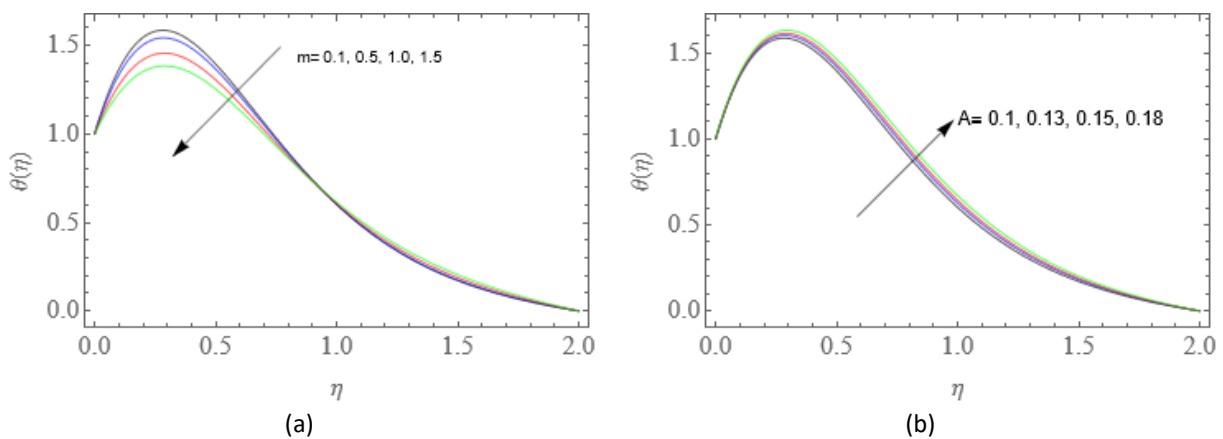


Fig. 8. Variation in $\theta(\eta)$ for increasing values of m and A

Figure 9 to Figure 13 demonstrate how various significant parameters affect temperature behaviour. Due to the fact that the temperature distribution is inversely proportional to the radiative parameter R , as seen in Figure 9, the temperature increases close to the boundary and then decreases thereafter. Figure 10 illustrates that when the Prandtl number grows, the temperature rises in the vicinity of the boundary before decreasing. Pr stands for the thermal diffusion to viscous diffusion ratio. Figure 11 illustrates how the temperature profile exhibits a rising trend when the temperature ratio tr increases. As a matter of fact, the temperature behaviour at the surface divided by the temperature behaviour beyond it is represented by tr . Additionally, the impact of Ec on the temperature field $\theta(\eta)$ is depicted in Figure 12. This graph shows that the temperature field $\theta(\eta)$ increases along with improved Ec estimates. Lastly, Figure 13 illustrates how the thickness of the thermal boundary layer rises in parallel with an increase in the heat source or sink parameter Q .

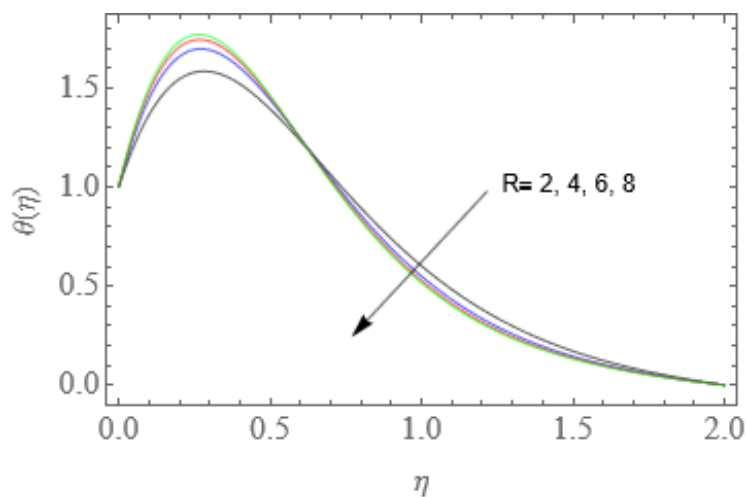


Fig. 9. Variation in $\theta(\eta)$ for increasing values of R

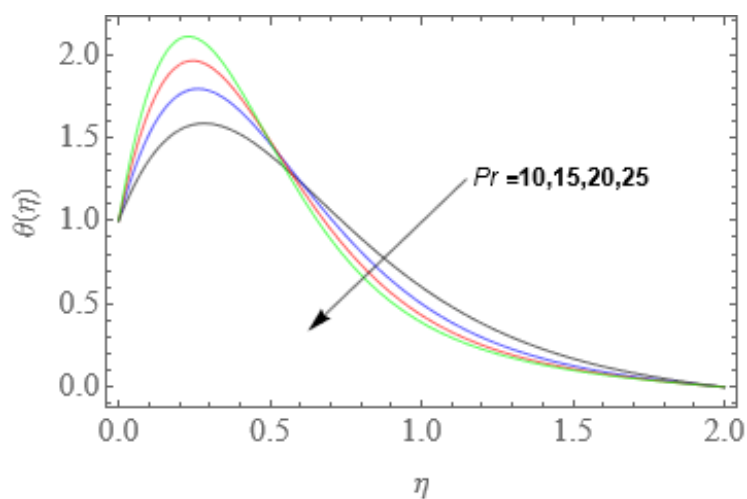


Fig. 10. Variation in $\theta(\eta)$ for increasing values of Pr

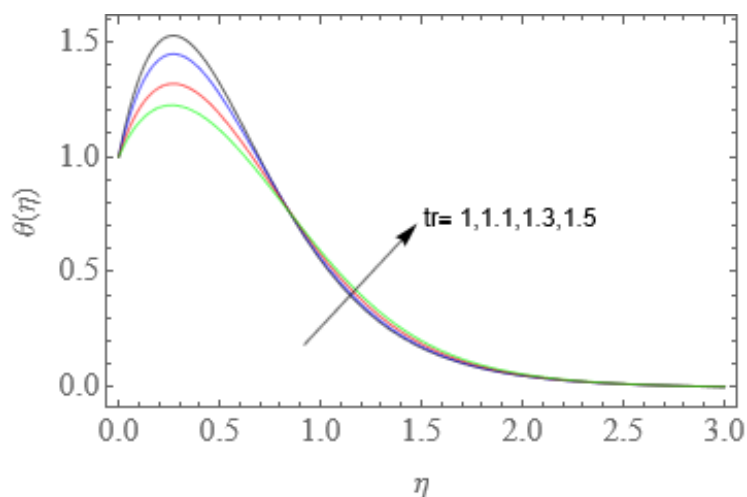


Fig. 11. Variation in $\theta(\eta)$ for increasing values of tr

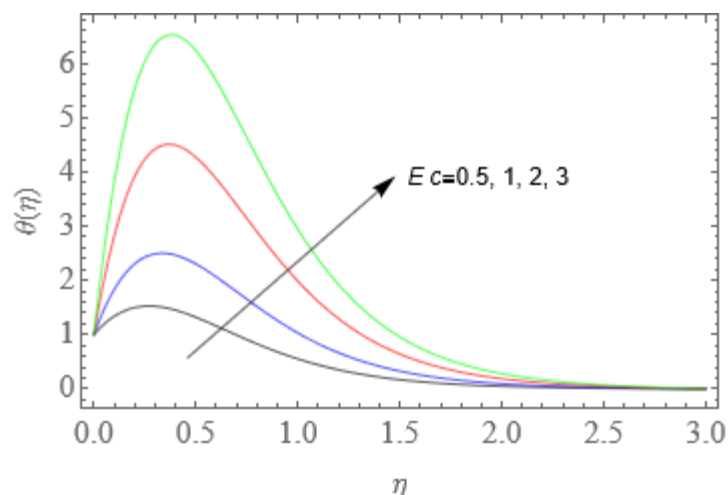


Fig. 12. Variation in $\theta(\eta)$ for increasing values of Ec

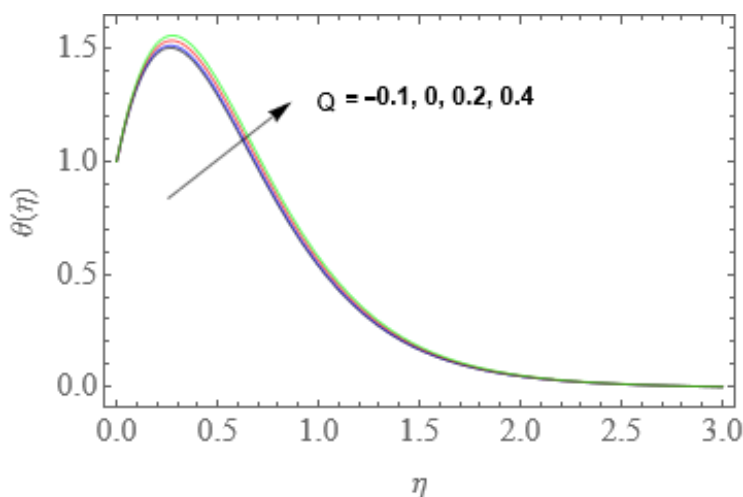


Fig. 13. Variation in $\theta(\eta)$ for increasing values of Q

5. Conclusion

In this article, a mathematical model has been presented for the influence of viscous dissipation and heat source/sink on an unsteady three dimensional Casson fluid flow through a stretching sheet. Using the similarity transformations, a set of ordinary differential equations has been derived for the boulder layer governing equations. These non-linear, coupled differential equations have been solved under valid boundary conditions using Matlab.

The results of this investigation are shown below.

- i. In Casson fluid, the velocity behaviour reduces along the x - axis as a result of increasing magnetic parameter M values.
- ii. Increasing the magnetic parameter M also results in an improvement in the Casson fluid's temperature behaviour.
- iii. The ascending values of Hall current m are responsible for the increment in velocity in the z direction and marginal increment is noticed in the x direction. However, the Casson fluid's temperature profile shows a little decline.
- iv. Because of the ascending values of unsteadiness A , a decrease in velocity behaviour is seen. However, the velocity profile of the Casson fluid does not significantly alter in the x direction.

- v. The increasing values of unsteadiness A in the Casson fluid are causing an increase in the temperature behaviour.
- vi. As the viscous dissipation Ec increases, a rise in temperature is observed.
- vii. Temperature profiles are enhanced as the heat source or sink parameter Q increases.
- viii. As viscous dissipation and the heat source or sink parameter rise, so does the rate of heat transfer coefficient.
- ix. The fluid flow model described in this study finds use in the printing industry, polymer engineering, blood flow and silicon suspensions. This work can be extended in future with some other geometries and physical conditions.

Acknowledgement

We are thankful to the reviewers for dedicating their time to read our article. We truly value your insightful comments and suggestions, which have significantly enhanced the quality of the content. This research was not funded by any grant.

References

- [1] Crane, Lawrence J. "Flow past a stretching plate." *Zeitschrift für angewandte Mathematik und Physik ZAMP* 21 (1970): 645-647. <https://doi.org/10.1007/BF01587695>
- [2] Pop, Ioan, and Tsung-Yen Na. "Unsteady flow past a stretching sheet." *Mechanics Research Communications* 23, no. 4 (1996): 413-422. [https://doi.org/10.1016/0093-6413\(96\)00040-7](https://doi.org/10.1016/0093-6413(96)00040-7)
- [3] Elbasha, Elsayed M. A. "Heat transfer over a stretching surface with variable surface heat flux." *Journal of Physics D: Applied Physics* 31, no. 16 (1998): 1951. <https://doi.org/10.1088/0022-3727/31/16/002>
- [4] Salleh, Mohd Zuki, Roslinda Nazar, and I. Pop. "Boundary layer flow and heat transfer over a stretching sheet with Newtonian heating." *Journal of the Taiwan Institute of Chemical Engineers* 41, no. 6 (2010): 651-655. <https://doi.org/10.1016/j.jtice.2010.01.013>
- [5] Misra, Mamta, Naseem Ahmad, and Zakawat Ullah Siddiqui. "Unsteady Boundary Layer Flow past a Stretching Plate and Heat Transfer with Variable Thermal Conductivity." *World Journal of Mechanics* 2, no. 1 (2012): 35-41. <https://doi.org/10.4236/wjm.2012.21005>
- [6] Grubka, L. J., and K. M. Bobba. "Heat transfer characteristics of a continuous stretching surface with variable temperature." *Journal of Heat Transfer* 107, no. 1 (1985): 248-250. <https://doi.org/10.1115/1.3247387>
- [7] Kamran, Muhammad. "Heat source/sink and Newtonian heating effects on convective micropolar fluid flow over a stretching/shrinking sheet with slip flow model." *International Journal of Heat & Technology* 36, no. 2 (2018): 473-482. <https://doi.org/10.18280/ijht.360212>
- [8] Anuar, Nur Syazana, Norfifah Bachok, and Ioan Pop. "Radiative hybrid nanofluid flow past a rotating permeable stretching/shrinking sheet." *International Journal of Numerical Methods for Heat & Fluid Flow* 31, no. 3 (2021): 914-932. <https://doi.org/10.1108/HFF-03-2020-0149>
- [9] Reddy, K. Veera, G. Venkata Ramana Reddy, Ali Akgül, Rabab Jarrar, Hussein Shanak, and Jihad Asad. "Numerical solution of MHD Casson fluid flow with variable properties across an inclined porous stretching sheet." *AIMS Mathematics* 7, no. 12 (2022): 20524-20542. <https://doi.org/10.3934/math.20221124>
- [10] Faraz, Faraz, Sajjad Haider, and Syed Muhammad Imran. "Study of magneto-hydrodynamics (MHD) impacts on an axisymmetric Casson nanofluid flow and heat transfer over unsteady radially stretching sheet." *SN Applied Sciences* 2 (2020): 1-17. <https://doi.org/10.1007/s42452-019-1785-5>
- [11] Sarma, Gobburu Sreedhar, Ganji Narendra, and Kamatam Govardhan. "Radiation effect on the flow of Magneto Hydrodynamic nanofluids over a stretching surface with Chemical reaction." *Journal of Computational Applied Mechanics* 53, no. 4 (2022): 494-509.
- [12] Hayat, T., A. Shafiq, A. Alsaedi, and S. A. Shahzad. "Unsteady MHD flow over exponentially stretching sheet with slip conditions." *Applied Mathematics and Mechanics* 37 (2016): 193-208. <https://doi.org/10.1007/s10483-016-2024-8>
- [13] Khan, Waqar Azeem, Muhammad Waqas, Wathek Chammam, Zeeshan Asghar, Ubaid Ahmed Nisar, and Syed Zaheer Abbas. "Evaluating the characteristics of magnetic dipole for shear-thinning Williamson nanofluid with thermal radiation." *Computer Methods and Programs in Biomedicine* 191 (2020): 105396. <https://doi.org/10.1016/j.cmpb.2020.105396>

- [14] Tabrez, M., and Waqar Azeem Khan. "Exploring physical aspects of viscous dissipation and magnetic dipole for ferromagnetic polymer nanofluid flow." *Waves in Random and Complex Media* (2022): 1-20. <https://doi.org/10.1080/17455030.2022.2135794>
- [15] Sarma, Gobburu Sreedhar, Ganji Narender, Dontula Shankaraiah, Vishwaroju Ramakrishna, and Gade Mallikarjun Reddy. "Analysis of Magneto Hydrodynamic Casson Nanofluid on an Inclined Porous Stretching Surface with Heat Source/Sink and Viscous Dissipation Effects: A Buongiorno Fluid Model Approach." *Journal of Advanced Research in Fluid Mechanics and Thermal Sciences* 109, no. 2 (2023): 151-167. <https://doi.org/10.37934/arfmts.109.2.151167>
- [16] Naganthran, Kohilavani, and Roslinda Nazar. "Unsteady boundary layer flow of a Casson fluid past a permeable stretching/shrinking sheet: paired solutions and stability analysis." In *Journal of Physics: Conference Series*, vol. 1212, no. 1, p. 012028. IOP Publishing, 2019. <https://doi.org/10.1088/1742-6596/1212/1/012028>
- [17] Krishanan, R., S. Maity, and B. S. Dandapat. "Unsteady flow of Casson liquid film on a stretching sheet with radiative heat transfer." *Surface Review and Letters* 27, no. 09 (2020): 1950204. <https://doi.org/10.1142/S0218625X19502044>
- [18] Hafidzuddin, Mohd Ezad Hafidz, Roslinda Nazar, Norihan M. Arifin, and Ioan Pop. "Unsteady flow and heat transfer over a permeable stretching/shrinking sheet with generalized slip velocity." *International Journal of Numerical Methods for Heat & Fluid Flow* 28, no. 6 (2018): 1457-1470. <https://doi.org/10.1108/HFF-11-2016-0440>
- [19] Mohd Sohut, Noor Farizza Haniem, Siti Khuzaimah Soid, Sakhinah Abu Bakar, and Anuar Ishak. "Unsteady three-dimensional flow in a rotating hybrid nanofluid over a stretching sheet." *Mathematics* 10, no. 3 (2022): 348. <https://doi.org/10.3390/math10030348>
- [20] Takhar, H. S., Ali J. Chamkha, and G. Nath. "Unsteady flow and heat transfer on a semi-infinite flat plate with an aligned magnetic field." *International Journal of Engineering Science* 37, no. 13 (1999): 1723-1736. [https://doi.org/10.1016/S0020-7225\(98\)00144-X](https://doi.org/10.1016/S0020-7225(98)00144-X)
- [21] Chamkha, Ali J., and Ali Al-Mudhaf. "Unsteady heat and mass transfer from a rotating vertical cone with a magnetic field and heat generation or absorption effects." *International Journal of Thermal Sciences* 44, no. 3 (2005): 267-276. <https://doi.org/10.1016/j.ijthermalsci.2004.06.005>
- [22] Chamkha, A. J., and S. E. Ahmed. "Similarity Solution for Unsteady MHD Flow Near a Stagnation Point of a Three-Dimensional Porous Body with Heat and Mass Transfer, Heat Generation/Absorption and Chemical Reaction." *Journal of Applied Fluid Mechanics* 4, no. 2 (2012): 87-94. <https://doi.org/10.36884/jafm.4.02.11921>
- [23] Anwar, Talha, Poom Kumam, and Wiboonsak Watthayu. "Unsteady MHD natural convection flow of Casson fluid incorporating thermal radiative flux and heat injection/suction mechanism under variable wall conditions." *Scientific Reports* 11, no. 1 (2021): 4275. <https://doi.org/10.1038/s41598-021-83691-2>
- [24] Hussain, Z., and Waqar Azeem Khan. "Impact of thermal-solutal stratifications and activation energy aspects on time-dependent polymer nanofluid." *Waves in Random and Complex Media* (2022): 1-11. <https://doi.org/10.1080/17455030.2022.2128229>
- [25] Khan, Waqar Azeem. "Impact of time-dependent heat and mass transfer phenomenon for magnetized Sutterby nanofluid flow." *Waves in Random and Complex Media* (2022): 1-15. <https://doi.org/10.1080/17455030.2022.2140857>
- [26] Ashraf, Samina, Muhammad Mushtaq, Kanwal Jabeen, Saadia Farid, and Rana Muhammad Akram Muntazir. "Heat and mass transfer of unsteady mixed convection flow of Casson fluid within the porous media under the influence of magnetic field over a nonlinear stretching sheet." *Proceedings of the Institution of Mechanical Engineers, Part C: Journal of Mechanical Engineering Science* 237, no. 1 (2023): 20-38. <https://doi.org/10.1177/09544062221110397>
- [27] Khader, M. M., M. Inc, and A. Akgul. "Numerical appraisal of the unsteady Casson fluid flow through Finite Element Method (FEM)." *Scientia Iranica* 30, no. 2 (2023): 454-463. <https://doi.org/10.24200/sci.2022.60176.6644>
- [28] Khalid, Asma, Ilyas Khan, Arshad Khan, and Sharidan Shafie. "Unsteady MHD free convection flow of Casson fluid past over an oscillating vertical plate embedded in a porous medium." *Engineering Science and Technology, an International Journal* 18, no. 3 (2015): 309-317. <https://doi.org/10.1016/j.jestch.2014.12.006>
- [29] Shehzad, Sabir Ali, T. Hayat, and Ahmed Alsaedi. "Three-dimensional MHD flow of Casson fluid in porous medium with heat generation." *Journal of Applied Fluid Mechanics* 9, no. 1 (2015): 215-223. <https://doi.org/10.18869/acadpub.jafm.68.224.24042>
- [30] Govardhan, Kamatam, Ganji Narender, and G. Sreedhar Sarma. "Viscous dissipation and chemical reaction effects on MHD Casson nanofluid over a stretching sheet." *Malaysian Journal of Fundamental and Applied Sciences* 15, no. 4 (2019): 585-592. <https://doi.org/10.11113/mjfas.v15n4.1256>
- [31] Maleque, Kh Abdul. "MHD Non-Newtonian Casson fluid heat and mass transfer flow with exothermic/endothermic binary chemical reaction and activation energy." *American Journal of Heat and Mass Transfer* 3, no. 1 (2016): 166-185. <https://doi.org/10.7726/ajhmt.2016.1011>

- [32] Kataria, Hari, and Harshad Patel. "Heat and mass transfer in magnetohydrodynamic (MHD) Casson fluid flow past over an oscillating vertical plate embedded in porous medium with ramped wall temperature." *Propulsion and Power Research* 7, no. 3 (2018): 257-267. <https://doi.org/10.1016/j.jprr.2018.07.003>
- [33] Vijayaragavan, R., and S. Karthikeyan. "Hall current effect on chemically reacting MHD Casson fluid flow with dufour effect and thermal radiation." *Asian Journal of Applied Science and Technology* 2, no. 2 (2018): 228-245.
- [34] Loon, Yew Wai, Nor Azwadi Che Sidik, and Yutaka Asako. "Numerical Analysis of Fluid Flow and Heat Transfer Characteristics of Novel Microchannel Heat Sink." *Journal of Advanced Research in Numerical Heat Transfer* 15, no. 1 (2023): 1-23. <https://doi.org/10.37934/arnht.15.1.123>
- [35] Khan, W. A., H. Sun, M. Shahzad, M. Ali, F. Sultan, and M. Irfan. "Importance of heat generation in chemically reactive flow subjected to convectively heated surface." *Indian Journal of Physics* 95 (2021): 89-97. <https://doi.org/10.1007/s12648-019-01678-2>
- [36] Prashu, Prashu, and R. Nandkeolyar. "A numerical treatment of unsteady three-dimensional hydromagnetic flow of a Casson fluid with Hall and radiation effects." *Results in Physics* 11 (2018): 966-974. <https://doi.org/10.1016/j.rinp.2018.10.041>